Development of a Simulation Toolkit for Electrical Capacitance Tomography

J. H. Hong[1], J. Mohamad-Saleh[2]

School of Electrical & Electronic Engineering, Engineering Campus, Universiti Sains Malaysia, 14300 Nibong Tebal, Seberang Perai Selatan, Pulau Pinang.
[1]Email: jwo-haur@tm.net.my, Tel.: 04-5943780
[2] Email: jms@eng.usm.my, Tel.: 04-593 7788 ext 6027

ABSTRACT

This paper describes a software tool that implements a two-dimensional finite element (FE) model for the simulation of capacitance readings from a specified electrical capacitance tomography (ECT) system. The simulation provides sensitivity distribution of the ECT system, and, with further development in the future, it will be integrated as a module in an image reconstruction tool. This software tool is developed on the MATLAB platform. The results and discussions are presented regarding sensitivity distributions simulated from a 12-electrode system and an 8-electrode system, and the inherent inaccuracy in these data. Conclusions are presented regarding validity of the present results and the direction of further research.

Keywords: Electrical Capacitance Tomography, Finite Element Model, Sensitivity Distribution, Image Reconstruction, Computer Simulation.

1.0 INTRODUCTION

Tomography, in general, is a technique where energy packets (predominantly electromagnetic) are fired externally through a concealed process which researchers wish to study the internal substance distribution of, and recaptured (measured) on the other side. Based on how the various substances in the concealed process had altered or affected the nature of the energy packets, a deduction is made of the distribution of those substances in the concealed process.

This has been done with great success in the medical field to give us the various forms of axial scans (axial tomography). The "energy packets" successfully used include X-ray (for computerized axial tomography, CAT), radio wave and magnetic flux (for magnetic resonance imaging, MRI), positrons (for positron emission tomography, PET), ultrasound, and neutrons.

Quite different from medical tomography, process tomography, has been used primarily for industrial benefits. For instance, it is used to examine multi-component flow regimes in pipelines carrying crude oil from oil fields to refineries and pipelines transporting granular solids in chemical plants (Huang et al 1989; Thorn et al 1990), and examine flame patterns in combustion chambers (He et al 1994), had seen development in a markedly different direction, as will be discussed in the next section.

2.0 ELECTRICAL CAPACITANCE TOMOGRAPHY

Most of the energy packets used for medical tomography are not suitable for use in process tomography either because of portability problems (power requirement, equipment size, ease of setting up, etc.) or because these radiations are destructive to substances contained in the process to be examined. Therefore, instead of using "hard field" systems such as X-ray and positron emission, process tomography has also employed "soft field" systems such as electrical impedance tomography (EIT) and electrical capacitance tomography (ECT).

In electrical capacitance tomography (ECT), a set of driving-measuring electrodes are placed around a pipe or process chamber to be monitored. Electrical field is generated in

turn between pairs of electrodes to measure the capacitances between these electrode pairs. Based on these capacitance readings, a deduction is made as to what distribution of permittivity (and hence the distribution of substances) between the electrode pairs would result in the kind of capacitance readings. This deduced distribution of permittivity, plotted in grey-levels (or color-coded levels) as cross-section of the pipe or process chamber, would afford researchers a glimpse into the process concealed within.

The earliest ECT systems were developed to have 8 driving-measuring electrodes. Over the years that followed, subsequent hardware development and improvement in the ability of capacitance transducers to resolve very small capacitance (Huang et al 1992) has enable the design and implementation of a 12-electrode systems. The 66 independent capacitance measurements that a 12-electrode system is more than double of the 28 measurements an 8-electrode system makes, hence a 12-electrode system has been found to be capable of a resolution twice as refined as that of an 8-electrode system. Figure 1 illustrates the typical electrodes setup of a 12-electrode system (Xie et al, 1992).

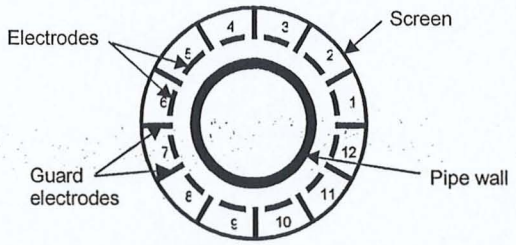

Figure 1: Typical electrodes setup of a 12-electrode ECT system.

In one complete measuring cycle, first, electrode 1 will drive with a potential, say, of magnitude V_C, while electrodes 2 to 12 (all set at ground potential) will measure the capacitance thus resulted. In the next measuring cycle, electrode 2 will drive the potential, while electrodes 3 to 12 will take the readings. Reading between electrode 2 and electrode 1 is not taken because this pair-up had been measured in the first round of measuring when electrode 1 was the source electrode. Similar strategy goes with the third round when electrode 3 is the source electrode: electrodes 4 to 12 will become the detecting electrodes, while reading between this and electrodes 1 and 2 are not repeated. Thus it goes when subsequent electrodes take up the role of source electrode, until the last round or measuring, when electrode 11 is the source electrode and electrode 12 the detecting electrode. This will be the last cycle, and it is no longer necessary for electrode 12 to drive the potential.

2.1. SIMULATION OF CAPACITANCE MEASUREMENTS

Poisson's equation expresses the relationship between dielectric constant (permittivity) distribution and the electrical field density within a certain space to the distribution of charges. With the assumption that the space within contains no free charges, Poisson's equation can be expressed as below (Reinecke et al, 1996; Xie et al, 1992):

$$\mathrm{div}\left(-\varepsilon_0 \varepsilon(x,y)\mathrm{grad}(\varphi(x,y))\right) = 0 \tag{1}$$

In the equation (1), ε_0 is the free space permittivity, $\varepsilon(x,y)$ is the permittivity at coordinates (x,y) and $\varphi(x,y)$ is the electrical potential at coordinates (x,y).

If $\varepsilon(x,y)$ and $\varphi(x,y)$ are both known, the capacitance readings between the electrodes can be solved using (Reinecke et al, 1996; Xie et al, 1992):

$$C = \frac{\varepsilon_0 \oint\!\!\!\oint_A \varepsilon(x,y)\mathrm{grad}(\varphi(x,y))\,\mathrm{d}A}{V_C} \tag{2}$$

In a simulation, it can be assumed that the permittivity distribution is known, that is, $\varepsilon(x,y)$ is known; however, due to the fact that this distribution is very irregular in general, the potential distribution, $\varphi(x,y)$, cannot be determined analytically.

Thus, $\varphi(x,y)$ needs to be solved numerically using the finite element (FE) method. The idea is to divide the area of electrical field into finite number of small elements (a process known as "meshing") of usually triangular shapes, of different sizes to accommodate the boundaries of substances. Then, with the sourcing potential as the boundary conditions, the potential distribution is solved from one node of a mesh triangle to another node considering the permittivity of the triangular mesh (Xie et al, 1992).

Once the solution of $\varphi(x,y)$ is obtained, equation (2) can be solved to yield the capacitance measurements according to the specified permittivity distribution. The total number of ECT readings depends on the number of electrodes used in the system. This can be determined using the equation below (Xie et al 1992):

$$N = \frac{n(n-1)}{2} \tag{3}$$

where N is the number of readings, while n is the number of electrodes in the system. For example, for a 12-electrode system, there would be 66 capacitance readings.

3. SIMULATION OF SENSITIVITY DISTRIBUTION

For this work, the PDE toolbox of MATLAB is used as the main processing muscle to generate the mesh for a user-specified decomposed geometry describing the permittivity distribution, and also to solve for the electric potential distribution based on the Dirichlet boundary conditions (Xie et al 1992). These results are then used to solve for the capacitance measurements as discussed in equation (2).

Figure 2(a) illustrates representation of a pipe with half-filled stratified flow of a two-component flow (gas, with relative permittivity 1.0, and oil, 2.6). The two rings are, the outermost being the screen electrode, and the inner one being the electrode-ring. Figure 2(b) shows the meshing performed on the flow regime of Figure 2(a) using the meshing commands of MATLAB.

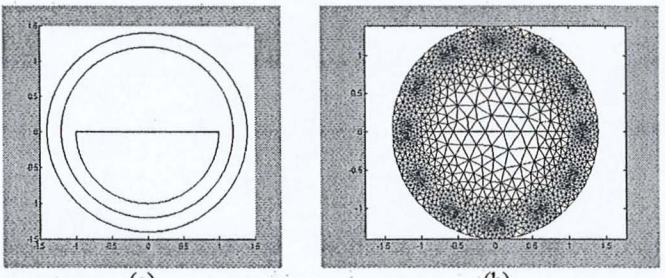

(a) (b)

Figure 2: (a) Two-component stratified flow, with the pipe half-filled.
(b) The mesh triangles formed for implementing FE solution.

Depending on the path of electrical field lines between an active pair of electrodes, the sensitivity of said electrode pair would not be uniform at every location within the area of measurement. It is essential for the process of image reconstruction that the sensitivity distribution of different electrode pairs should be determined.

Supposing the area of measurement is taken as a square encompassing the pipe, and this area of measurement is divided into 30 × 30 square pixels (900 pixels), the sensitivity at pixel k between two electrodes i and j, denoted $S_{ij}(k)$, is defined as (Isaksen, 1996):

$$S_{ij}(k) = \frac{C_{ij}^{(oil,k)} - C_{ij}^{gas}}{C_{ij}^{oil} - C_{ij}^{gas}} \times \frac{1}{\varepsilon_{oil} - \varepsilon_{gas}} \times \frac{A_{\max}}{A_k} \quad (4)$$

C_{ij}^{gas} is the capacitance reading between electrodes i and j when the whole pipe is filled with only gas, while C_{ij}^{oil} is when the whole pipe is filled with only oil. $C_{ij}^{(oil,k)}$ is the capacitance reading between electrodes i and j when mesh element k alone is filled with oil, while the rest of the pipe is filled with gas. ε_{oil} and ε_{gas} are the relative permittivity of oil and gas respectively. A_{max} is the maximum area of a single pixel, while A_k is the area of pixel k. For the case of uniform square pixels, these two values should be the same, thus rendering the ratio always one. But in cases where a square pixel is partially considered, this ratio had to be calculated accordingly.

4. RESULTS AND DISCUSSION

For a 900-pixel imaging system, with 12 electrodes, the sensitivity distribution obtained should be a 900×66 matrix, corresponding to 900 pixels, each having 66 ECT values. On the other hand, for an 8-electrode system, the sensitivity distribution is a 900×28 matrix.

Assuming that all electrodes used are identical and driven at exactly the same potential, there should only be 6 unique sensitivity distributions for a 12-electrode system, as shown in Figure 3, and only 4 unique sensitivity distributions for a 8-electrode system, as shown in Figure 4. Take the 12-electrode system for example: the sensitivity distribution between electrode 1 and electrode 3 should be the same as the sensitivity distribution between electrode 7 and electrode 9, because in both cases, the driving electrode and the measuring electrode are separated by 1 electrode.

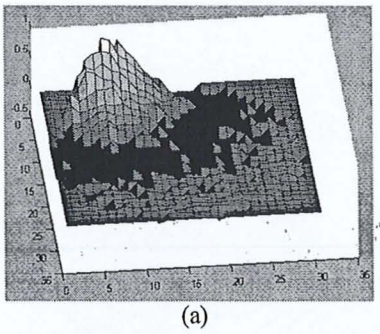

(a)

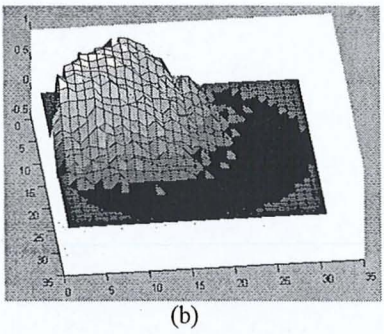

(b)

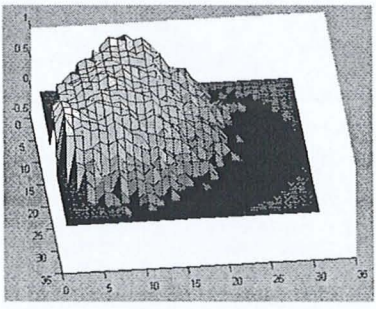

(c)

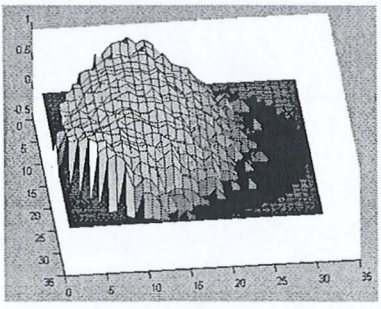

(d)

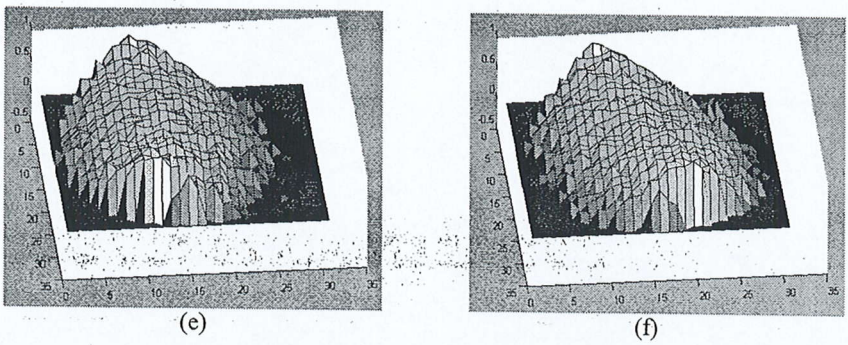

(e) (f)

Figure 3: Sensitivity distribution (a) between adjacent electrodes; (b) between electrodes set 1 electrode apart; (c) 2 electrodes apart; (d) 3 electrodes apart; (e) 4 electrodes apart; (f) 5 electrodes apart.

Take for example, the sensitivity distribution between two electrodes set apart by 1 electrode as shown in Figure 3(b) indicates bright elevated area (this is the sensitive region between the driving and measuring electrodes) occupying about a quarter of the circle, and dark recessed area (this is the region where the two electrodes are not sensitive to). What this distribution of sensitivity means is, if an object of markedly different permittivity is located in the region of bright elevated pixels, it would have more prominent effect on the capacitance reading between the two electrodes, than if it were located in the region of dark recessed pixels.

Similar simulation has been carried out on an 8-electrode system, which has only 4 unique sets of sensitivity distribution, and the results are recorded in Figure 4.

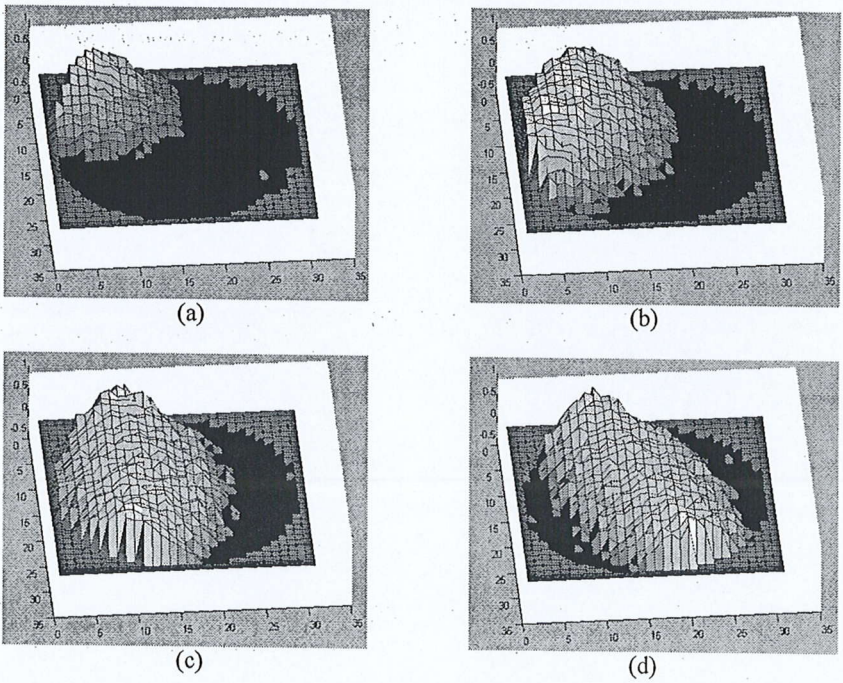

(a) (b)

(c) (d)

Figure 4: Sensitivity distribution (a) between adjacent electrodes; (b) between electrodes set 1 electrode apart; (c) 2 electrodes apart; (d) 3 electrodes apart.

Inherent in these sensitivity distributions is a potential problem that might adversely affect the accuracy of image reconstruction, that is, the non-linearity of the sensitivity

data. Summing along the rows of the sensitivity distribution matrix, $\mathbf{S}_n$, we would a 900×1 matrix, **W**, which represents the weighting factors for the grey level of each of the 900 pixels (Xie et al, 1992). Figure 5 shows the graphic visualization of the weighting factors posed by sensitivity distribution of the 12-electrode system discussed above. The weighting factors for the 8-electrode system are not shown here, but they are similar in nature and the effects they would have on reconstructed image.

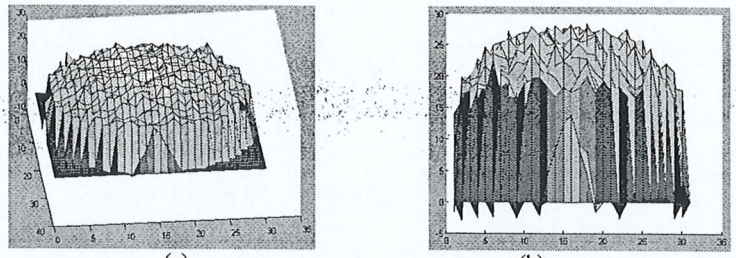

(a) (b)

Figure 5: Weighting factor for the reconstructed grey level;
(a) isometric view; (b) side view.

It can be seen from the visualization of Figure 5 that the weight is accentuated at the center. Weighting can be understood as amplification of grey level. What the distribution in Figure 5 will provide is higher "amplification" for grey levels (including invalid levels) at the accentuated regions (that is, the center). The possible adverse effect this might have when these sensitivity distribution data are used in the image reconstruction process is that it might erroneously over-amplify the grey level of pixels at the centre (this is analogous to the case of an amplifier with too big a bandwidth picking up noise signals from unwanted frequency range).

5. CONCLUSIONS

This ECT simulation toolkit that is being developed has thus far produced simulated sensitivity distributions that are in agreement with results from other researches (Xie et al 1992, Isaksen 1996, Xie et al 1989). The non-linearity problem discussed above can be overcome in the greater part by imposing counter weights inversely proportional to the inherent weighting factors. The next stage of research will involve the reconstruction of flow image using the sensitivity distribution data obtained herein. Works on simulation of sensitivity distributions is far from being over and done with; many revisits of the methodology employed and attempts at correction of the non-linearity problem are expected as subsequent works on image reconstruction will inevitably encounter problems of inaccurate reconstructed images that sometimes find their roots in the inaccuracy of the sensitivity distributions. It may sound counter-productive not to attempt to correct all possible inherent inaccuracy in the sensitivity distribution data proactively before work begins on image reconstruction. Nevertheless, some of these inaccuracies would not be apparent until the data are actually used for image reconstruction. Hence, in greater part, the attempt at perfecting the simulation of sensitivity distribution would have to go hand-in-hand with works on image reconstruction software modules.

REFERENCES

Huang, S. M., Plaskowski, A., Xie, C. G., and Beck, M. S. (1989). "Tomographic imaging of two-component flow using capacitance sensor". J. Phys. E, 22(3), 173-177.

Thorn, R., Huang, S. M., Xie, C. G., Salkeld, J. A., Hunt, A., and Beck, M. S. (1990). "Flow imaging for multi-component flow measurement'. Flow Meas. Instrum., 139(1), 83-88.

He, R., Beck, C. M., Waterfall, R. C., and Beck, M. S. (1994). "Finite Element Modelling and Experimental Study of Combustion Phenomena Using Capacitance Measurement". Process Tomography – A Strategy for Industrial Exploitation, 367-376.

Huang, S. M., Xie, C. G., Thorn, R., Snowden, D., and Beck, M. S. (1992). "Design of sensor electronics for electrical capacitance tomography". IEE Proceedings-G, 139(1), 83-88.

Xie, C.G., Huang, S. M., Hoyle, B. S., Thorn, R., Lenn, C., Snowden, D., and Beck, M. S. (1992). "Electrical capacitance tomography for flow imaging: system model for development of image reconstruction algorithms and design of primary sensors". IEE Proceedings-G, 139(1), 89-98.

Reinecke, N., and Mewes, D. (1996). "Recent developments and industrial/research applications of capacitance tomography". Meas. Sci. Technol., 7(1996), 233-246.

Isaksen, Ø. (1996). "A review of reconstruction techniques for capacitance tomography". Meas. Sci. Technol., 7(1996), 325-337.

Xie, C. G., Plaskowski, A., Beck, M. S. (1989) "8-electrode capacitance system for two-component flow identification – Part 1: Tomographic flow imaging". IEE Proceedings, 136(4), 173-183.